IOP Publishing Journal of Physics: Condensed Matter
J. Phys.: Condens. Matter **27** (2015) 035104 (8pp) doi:10.1088/0953-8984/27/3/035104

Sub-diffusive electronic transport in a DNA single-strand chain with electron–phonon coupling

M O Sales[1], M L Lyra[1], F A B F de Moura[1], U L Fulco[2] and E L Albuquerque[2]

[1] Instituto de Física, Universidade Federal de Alagoas, 57072-900 Maceió-AL, Brazil
[2] Departamento de Biofísica e Farmacologia,Universidade Federal do Rio Grande do Norte, 59072-970 Natal-RN, Brazil

E-mail: fidelis@fis.ufal.br

Received 2 November 2014, revised 9 December 2014
Accepted for publication 15 December 2014
Published 7 January 2015

Abstract

We investigate the electronic wavepacket dynamics in a finite segment of a DNA single-strand chain considering the electron–phonon coupling. Our theoretical approach makes use of an effective tight-binding Hamiltonian to describe the electron dynamics, together with a classical harmonic Hamiltonian to treat the intrinsic DNA vibrations. An effective time-dependent Schrödinger equation is then settled up and solved numerically for an initially localized wave-packet using the standard Dormand–Prince eighth-order Runge–Kutta method. Our numerical results indicate the presence of a sub-diffusive electronic wavepacket spread mediated by the electron–phonon interaction.

Keywords: localization, DNA, electron-lattice

(Some figures may appear in colour only in the online journal)

1. Introduction

Recent advances in physical and biochemical methods have strongly supported that biomolecules can be a proper medium for charge transport. Several studies aiming to characterize the current flow through double-strand DNA molecules connected with metal electrodes have suggested a wide range of regimes ranging from high electron mobilities to insulator behavior [1–7]. The observed distinct behaviors is intimately related to the characteristics of the contact with the electrodes, the environment, the mechanical stress, the molecular orientation, as well as upon the integrity of the molecule itself [8, 9]. In general, biostructures show complex topologies with high flexibility and many degrees of freedom [8]. The ability of biological organisms to manufacture such complex molecules is one of the main drivers of bio-electronics research. This important feature counterbalances with their low lifetime due to degradation, as well as their reactivity with water and other substances (for a recent review see [10]). Considering the growing technological interest in developing bio-electronic devices based on organic molecules [8], it is fundamental to deeply understand the charge transport through organic molecules, in special DNA, RNA and proteins. Along this direction, new mathematical and numerical methodologies are necessary to study these molecules due to their complexity when compared with the more traditional solid-state materials.

In determining the electronic properties of biomolecules, the molecular structure must be calculated, and a suitable transport theory must be used to describe the time evolution of the appropriate charge distribution. For the DNA molecule, the possibility of replicating and performing its biological function implies rapid structural dislocations, measured by dramatic nonlinear deformations leading to Anderson localization, i.e. to the exponential localization of the electronic states, and thus significant reduction of conductance [5–7, 10]. A theoretical description of these effects is usually carried out at the level of polaronic theories [11, 12], despite the dislocation's sufficiently high amplitude.

Interaction of a DNA electronic subsystem (considered in the one-band approximation) with the conformationally

active vibrational modes of the chain (considered as a symbolic sequence of a four letter alphabet, namely guanine-G, cytosine-C, adenine-A and thymine-T) is, in most cases, non-linear [13]. The electron-lattice coupling is mainly considered to describe the DNA electron interaction with the stretching/squeezing transversal harmonic vibrational modes of the DNA chain [14]. These dislocations can either occur in a synchronized manner (normal mode propagation) [15] or incoherently (thermal motion) [16–18].

In low-dimensional systems, like the majority of the biological molecules, the effect of nonlinearity seems to be dominant over the role played by disorder. For instance, the spreading of an initially localized wave-packet in a 1D discrete nonlinear Schrödinger lattice with disorder was recently studied, and it was observed that Anderson localization is suppressed and sub-diffusive dynamics takes place above a certain critical nonlinearity strength [19]. The electronic wave-packet dynamics in a twisted ladder geometry mimicking a DNA-like segment has also been addressed considering an electron–phonon interaction within the adiabatic approximation [20]. The results suggested a diffusive-like spread of the electronic wave-packet induced by the nonlinearity [21].

Tight-binding models describing the electronic wavepacket dynamics in DNA segments have been successfully accounted for the Anderson localization of the one-electron eigenstates [5–7, 10, 22, 23]. Due to the random distribution of the distinct bases, the electronic eigenstates remain exponentially localized on small segments of the DNA chain. Notwithstanding, the presence of some degree of correlation in the disorder distribution has a limited influence on the nature of these eigenstates [22]. Furthermore, simple models considering a single-strand DNA (ss-DNA) molecule are able to capture the main aspects related to the disorder effect on the nature of the electronic states [22, 23]. On the other hand, as far as the vibrational modes of a DNA molecule are concerned, the effective spring constant between neighboring bases mediated by the sugar-phosphate backbone is much larger than the spring constants between paired bases, i.e. the harmonic inter-strand coupling is much weaker than the intra-strand coupling [24]. Therefore, the main influence of the electron-lattice coupling in DNA segments is expected also to be well described by single-stranded models, avoiding the use of the more robust, although more physically and biologically relevant, double stranded DNA (ds-DNA) molecule.

Following the lines described above, it is the aim of this paper to study the dynamics of a one-electron wavepacket spreading in a single-strand DNA molecule in the presence of harmonic, as well as anharmonic vibrations associated with the bases displacements. The single-strand DNA chain contains four distinct values of the on-site potentials simulating the four bases of a DNA molecule. Further, we will take into account a direct coupling between the electron dynamics and the local vibrations. The electronic hopping energy will be assumed to depend on the effective distance between nearest-neighboring bases, increasing exponentially when the distance between neighboring bases decreases. By solving numerically the equations describing the dynamics for the electron and the lattice vibrations, we compute the spreading of an initially localized electronic wave-packet, whose solution suggests that the electron–phonon term considered here promotes a sub-diffusive spread for long times.

The plan of this work is as follows: in section 2 we present the effective tight-binding Hamiltonian together with the lattice Hamiltonian to describe the electronic motion. Section 3 depicts our main results with a detailed discussion of them. The conclusions are in section 4.

2. Model and formalism

Our basic theoretical model makes use of an effective tight-binding Hamiltonian describing one electron moving in a DNA single-strand segment with N bases, coupled to the lattice harmonic vibrations, whose expression is given by [25]:

$$H = H_{\text{lattice}} + \sum_{n=1}^{N}\Big[V_{n+1,n}(c_{n+1}^{\dagger}c_n) + V_{n,n-1}(c_n^{\dagger}c_{n-1})\Big] + \sum_{n=1}^{N}\epsilon_n c_n^{\dagger}c_n. \quad (1)$$

Here, $V_{n\pm1,n}$ is the electronic hopping term between two adjacent nucleotides, whose ionization energies at site n are defined by ϵ_n. Also, H_{lattice} represents the classical Hamiltonian describing the lattice harmonic vibrations:

$$H_{\text{lattice}} = \sum_{n=1}^{N}\frac{P_n^2}{2m_n} + \frac{1}{4}\Big[\beta_n Q_+^2 + \beta_{n-1}Q_-^2\Big], \quad (2)$$

with $Q_+ = Q_{n+1} - Q_n$ and $Q_- = Q_n - Q_{n-1}$. P_n and Q_n are the classical momentum and displacement coordinates of the DNA's bases (G, C, A, and T) at site n. In this approach, we will consider all elastic forces constants, i.e. $\beta_n = \beta_{n-1} = \beta$. The ionization energies at site n, ϵ_n, will be constructed as follows: initially we consider an uncorrelated random sequence containing four distinct values of the on-site ionization energies mimicking the sequence of the DNA's bases. For the on-site energies we used the values $\epsilon_G = 7.75$, $\epsilon_C = 8.87$, $\epsilon_A = 8.24$, and $\epsilon_T = 9.14$, all units in eV [10]. The fraction of each base is taken to be the same one found in the firstly sequenced human chromosome 22 (Ch 22), entitled NT_{011520}, whose number of letters is about 3.4×10^6 nucleotides. This sequence was retrieved from the internet page of the National Center of Biotechnology Information. However, we would like to stress that the exact sequence of bases of NT_{011520} is not relevant to the general dynamical behavior we intend to explore, as long as the bases used for the calculation comprise each base (G, C, A, and T) to provide mass disorder. The mass distribution m_n will be the masses of the four distinct bases, considering all masses in units of the cytosine mass (M_C), i.e.: $m_A = M_A/M_C = 135.13/111.10$, $m_G = M_G/M_C = 151.13/111.10$, $m_T = M_T/M_C = 126.11/111.10$, and $m_C = 1$.

The interaction between the electron and the vibrational modes in our model relates the electronic hopping term $V_{n+1,n}$

with the displacement coordinates of the sites from their equilibrium positions [26–29]:

$$V_{n+1,n} = -\exp[-\alpha Q_+]. \tag{3}$$

The coefficient α defines how the electronic hopping term $V_{n+1,n}$ depends on the relative displacement of the lattice units, i.e. it determines the electron–phonon coupling strength. Accordingly to [27–29], the exponential form of the hopping term $V_{n+1,n}$ stands for both small and large relative displacement, thus going beyond the range of interactions considered in the SSH (Su–Schrieffer–Heeger) theory [30–33]. For small relative displacements, we recover the SSH approximation

$$V_{n+1,n} \approx -[1 - \alpha(Q_{n+1} - Q_n)]. \tag{4}$$

We will follow the time evolution of an initially localized one-electron wave-packet. The time-dependent wave-function $|\Phi(t)\rangle$ can be obtained by the numerical solution of the time-dependent Schrödinger equation in which the electron is initially localized at site $N/2$, i.e.:

$$|\Phi(t=0)\rangle = \sum_n c_n(t=0)|n\rangle, \tag{5}$$

where

$$c_n(t=0) = \delta_{n,N/2}. \tag{6}$$

The Wannier amplitudes evolve in time according to the time-dependent Schrödinger equation as ($\hbar = 1$)

$$\mathrm{i}\frac{\mathrm{d}c_n(t)}{\mathrm{d}t} = \epsilon_n c_n(t) - \exp(-\alpha Q_+)c_{n+1}(t) - \exp(-\alpha Q_-)c_{n-1}(t). \tag{7}$$

In this system of units, time is given in units of $\hbar/\mathrm{eV} = 4.13 \times 10^{-15}$ s. Moreover, the lattice equation can be written as

$$m_n \frac{\mathrm{d}^2 Q_n(t)}{\mathrm{d}t^2} = \left[\beta_n Q_+ - \beta_{n-1} Q_-\right] - \alpha\Big[\exp(-\alpha Q_+)(c^*_{n+1}c_n + c_{n+1}c^*_n) - \exp(-\alpha Q_-)(c^*_n c_{n-1} + c_n c^*_{n-1})\Big] \tag{8}$$

In what follows the elastic constant will be in units of $m_C\,\mathrm{eV}^2/\hbar^2 = 1.06 \times 10^4\,\mathrm{N\,m^{-1}}$, the lattice displacement in Å, and α in units of $\mathrm{Å}^{-1}$. Our numerical formalism is based on the precise numerical solution of the previous equations (7) and (8). Both dynamic equations will be solved by using a standard Dormand–Prince eighth-order Runge–Kutta method monitoring the local truncation error [34, 35], with time step $\mathrm{d}t \approx 10^{-3}$. Aiming to characterize the dynamic behavior of the wave-packet, we compute typical quantities that can bring information about the electronic transport on this model, namely the participation function $\xi(t)$ and the wave-function spread $\sigma(t)$.

The participation function is defined by [36, 37]

$$\xi(t) = 1/\sum_n |c_n(t)|^4, \tag{9}$$

giving an estimation of the number of sites over which the wave-packet is spread at time t. In particular, the asymptotic participation function becomes size-independent for a localized wave-packet. On the other hand, $\xi(t \to \infty) \propto N$ corresponds to the regime where the wave-packet is distributed over the lattice [25, 36, 37].

The wave-packet mean-square displacement $\sigma(t)$ is defined by [38]

$$\sigma(t) = \sqrt{\sum_n (n - n_0)^2 |c_n(t)|^2}. \tag{10}$$

Note that $\sigma(t)$ varies from 0, for a wave-function confined to a site, to a term proportional to the number of sites, for a wave extended over the whole system.

We will also study the temporal auto-correlation function $C(t)$ defined by [38, 39]:

$$C(t) = \frac{1}{t}\int_0^t R(t')\mathrm{d}t', \tag{11}$$

where $R(t') = |c_{N/2}(t')|^2$ denotes the return probability. In the asymptotic limit $t \to \infty$, the temporal auto-correlation function vanishes as $C(t) \propto 1/t^\theta$, where θ represents, for $d = 1$, the exponent governing the size scaling of the time-independent participation function for low energies, i.e. $\xi(E \approx 0) \propto N^\theta$ [38, 39]. This scaling relation is a direct consequence of the fractal character of the eigenfunctions fluctuations [40, 41]. In the long time regime, the return probability saturates at a finite value whenever the wave-packet remains trapped in a finite region around the starting point. Otherwise, it vanishes as the wave-packet continuously spreads over the lattice [42]. Whenever the system presents a phase of truly extended states, the auto-correlation function vanishes linearly with $1/t$. A slower non-linear decay is usually a signature of an intermediate dynamical regime.

3. Results and discussions

Let us now present and discuss our main achievements. In order to avoid border effects when the wavepacket reaches the borders of a finite DNA segment, we performed our numerical calculations on a self-expanding chain. As a result, we measured the temporal evolution of a wavepacket initially located at the center of the self-expanding chain, i.e. $c_n(t = 0) = \delta_{n,N/2}$. When the probability of finding the electron at one of the ends of the chain exceeds 10^{-40}, fifteen new sites are added to them. In this way, one avoids eventual finite-size effects on the wavepacket dynamics. This technique has been successfully employed in previous studies of one-electron wavepacket dynamics and provides reliable results concerning the asymptotic spread of diffusing wavepackets [21, 33, 37, 44, 46]. The lattice equations were solved by considering an initial impulse excitation ($P_n = \delta_{n,N/2}$; $Q_n = 0$) according to [43]. We kept the wave-function norm within the limit $|1 - \sum_n |c_n(t)|^2| < 10^{-10}$ for all times considered, using 50 disorder configurations.

Initially, we plot in figures 1(*a*)–(*h*), the mean squared displacement $\sigma(t)$ and the participation number $\xi(t)$ for the

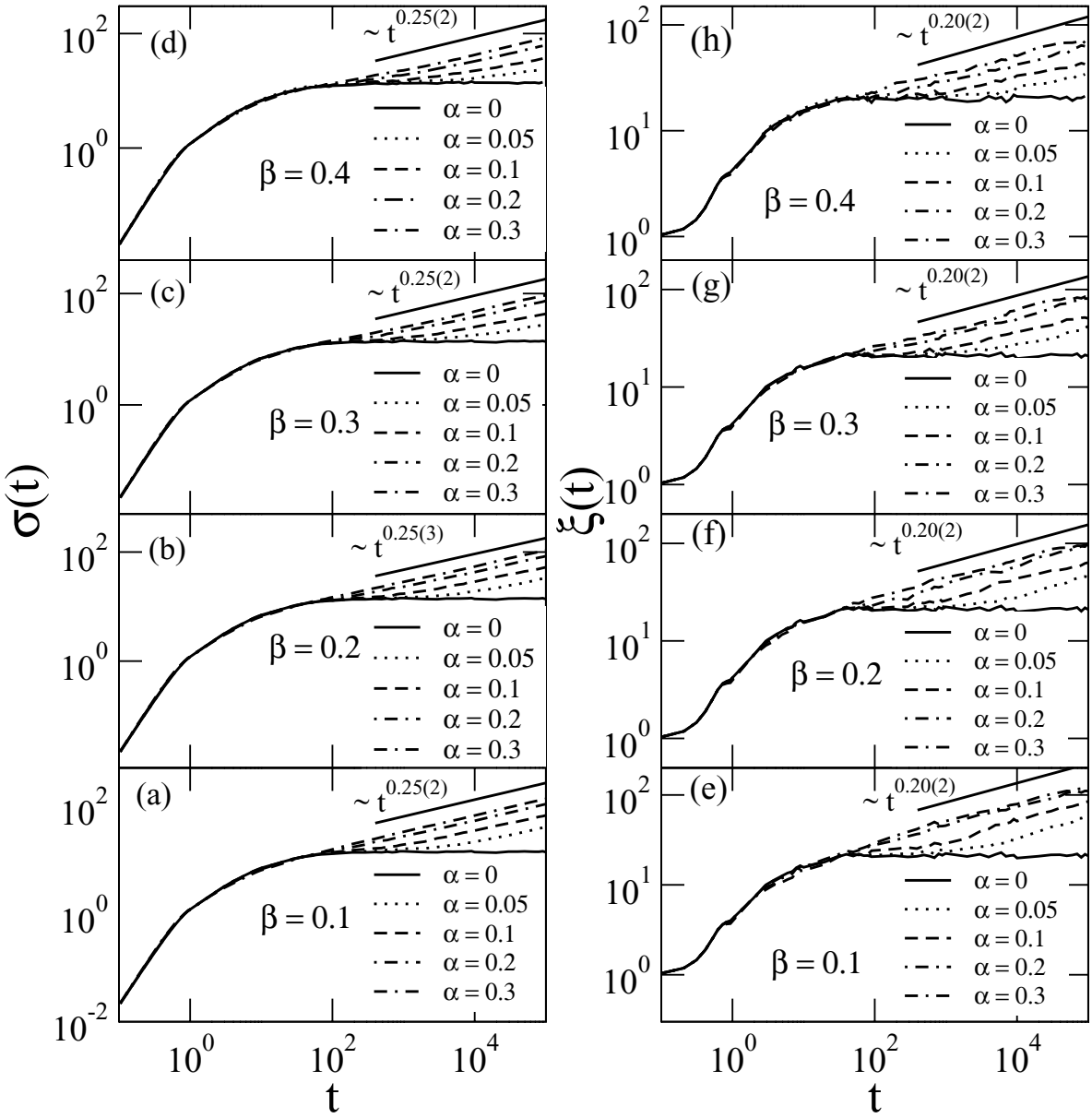

Figure 1. (*a*)–(*d*) Mean-square displacement $\sigma(t)$ and (*e*)–(*h*) participation function $\xi(t)$ (in units of the lattice spacing) versus time for several values of the off-diagonal electron–phonon coupling strength α, and spring constant β (all units are given in the text). Our numerical results indicate that off-diagonal nonlinearity ($\alpha > 0$) induces the sub-diffusive spreading of the wavepacket, leading to $\sigma(t) \propto t^{0.25(2)}$ and $\xi(t) \propto t^{0.20(3)}$ (the numbers in parenthesis stand for the fitting error bars).

following values of the electron–phonon coupling strength α: 0, 0.05, 0.1, 0.2, 0.3. We consider the spring constant β varying from 0.1 up to 0.4. In the absence of the non-linearity ($\alpha = 0$) we observe the well-known Anderson localization regime in which the wave-packet does not expand [37]. This behavior was stressed in details in [22, 23], including several kinds of diagonal DNA-like disorder. Moreover, figure 1 also shows the sub-diffusive regime that exists for $\alpha > 0$. By analyzing these data, we found that the mean-square displacement $\sigma(t)$ behaves like $t^{0.25(3)}$, while the participation function $\xi(t)$ has a temporal dependence $t^{0.20(3)}$. We emphasize that these results are in agreement with those found in [21], where it was verified a sub-diffusive behavior related to the nonlinear Schrödinger DNA equation for a twisted ladder geometry with an adiabatic electron–phonon interaction. However, in this previous work, the electron–phonon coupling was taken into account in the time-dependent Schrödinger equation through a cubic non-linearity (in the absence of any lattice equations), in such a way that the lattice vibrations and its coupling with the electronic dynamics were treated effectively by using a discrete nonlinear Schrödinger equation. Furthermore, a sub-diffusive regime was also found in discrete nonlinear Schrödinger models with off-diagonal non-linearity [44].

Our model considers two distinct sources of static disorder, namely: a disorder within the on-site energy distribution of DNA's bases (equation (7)), and also a disorder within the mass distribution of the bases (equation (8)). Therefore, both the tight-binding electron Hamiltonian and

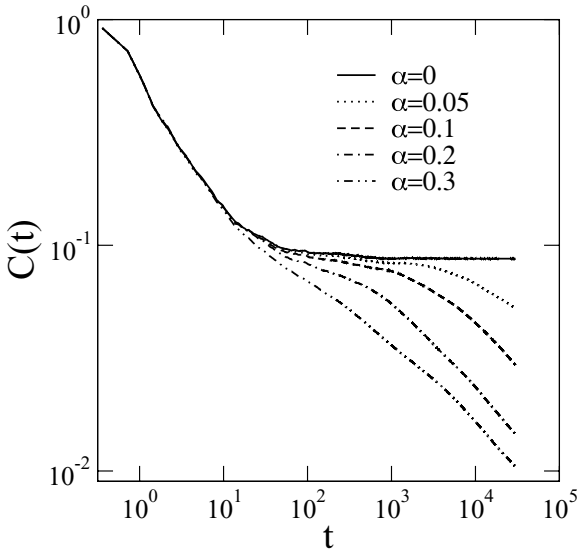

Figure 2. Temporal auto-correlation function $C(t)$ versus t for the electron–phonon coupling strength $\alpha = 0$ up to 0.3.

the classical Hamiltonian describing the lattice harmonic vibrations contain static disorder. Besides these sources of static disorder, the electron hopping amplitudes also dynamically change due to the coupling with the lattice vibrations. This feature adds a dynamical source of disorder to the electron propagation. Similarly, the electron propagation couples to the lattice displacements resulting in an effective dynamical disorder affecting the lattice vibrations. Our results suggest that even in the presence of these two static disorder distributions the electron–phonon term can promote electronic transport. We stress that this result evidences the consistence of the two formalisms, namely, the nonlinear discrete Schrödinger equation used in [21, 44] and the quantum-classical treatment considered in the present work.

In figure 2 we investigate the electronic dynamics within our DNA model by using the temporal auto-correlation function. Our calculations were done for the spring constant $\beta = 0.4$, with the electron–phonon coupling strength α varying from 0 up to 0.3. In the absence of the electron–phonon coupling ($\alpha = 0$) we observe that the auto-correlation function saturates at large time t. In this region, the static disorder of the DNA model, due to the two distinct sources described above, promotes the localization of the electronic wave-function. Therefore, the return probability at the large time t saturates at a finite value, meaning that the auto-correlations remain constant in time. For $\alpha > 0$ we observe a slow non-linear decay of the temporal auto-correlation function $C(t)$. For $\alpha > 0.1$ and for long times, we can estimate $C(t) \approx t^{-0.40(1)}$.

Formally, whenever the system presents a phase of truly extended states, the auto-correlation function vanishes linearly with $1/t$. In the present DNA model, our result showing a non-linear decay of $C(t)$ suggests that the eigenfunctions exhibit an intermediate nature between the fully localized and the extended states. In [38] it was investigated an electronic model with correlated disorder in which an intermediate dynamical regime non-ballistic was associated with the presence of weakly localized eigenfunctions. We emphasize that in our model we are unable to calculate directly these eigenfunctions due to the time-dependence of the hopping amplitudes. As a consequence, a comparison of the auto-correlation function exponent and the size scaling of the static participation number can not be drawn.

Next, we would like to stress the classical harmonic approximation imposed on the lattice harmonic vibrations depicted in equation (2), which was also considered in several previous works [21, 30, 44]. In a vibrating system, the harmonic approximation takes into account only those with small amplitude. Therefore, some thermal effects can promote strong vibrations and an anharmonic treatment could be important. In view of that, let us analyze briefly the effect of nonlinear atomic forces on our results. We rewrite the lattice Hamiltonian (equation (2)) in order to include an anharmonic cubic force yields:

$$H^{*}_{\text{lattice}} = H_{\text{lattice}} + (\eta/6)\sum_{n}\left(Q_{+}^{3} + Q_{-}^{3}\right), \qquad (12)$$

where η represents the strength of the cubic non-linearity considered in the model. The quantum Schrödinger equation (7) remains unchanged, and the lattice equation needs to be rewritten in order to include the anharmonic term, yielding:

$$\begin{aligned} m_n \frac{\mathrm{d}^2 Q_n(t)}{\mathrm{d}t^2} = &\left[\beta_n Q_+ - \beta_{n-1} Q_-\right] + \eta\left[Q_+^2 - Q_-^2\right] \\ &-\alpha\Big[\exp(-\alpha Q_+)(c^*_{n+1}c_n + c_{n+1}c^*_n) \\ &-\exp(-\alpha Q_-)(c^*_n c_{n-1} + c_n c^*_{n-1})\Big]. \end{aligned} \qquad (13)$$

In what follows, η will be given in units of $m_c\,\mathrm{eV}^2/\hbar^2\,\text{Å} = 1.06 \times 10^{-6}\,\mathrm{N\,m^{-2}}$. Figures 3(*a*) and (*b*) summarize our calculations in the presence of the anharmonicity. We consider the spring constant $\beta = 0.4$, and the electron–phonon coupling $\alpha = 0.3$ (this value was the highest intensity we were able to proceed with our numerical calculations within the desired accuracy). We observe that the wave-packet width $\sigma(t)$ diverges in a sub-diffusive way ($\sigma \propto t^{0.25(2)}$) similar to that observed in the absence of anharmonicity ($\eta = 0$). Moreover, the temporal auto-correlation function (see figure 3(*b*)) vanishes in a similar way to our calculations for $\eta = 0$, suggesting that even in the presence of a weak cubic anharmonicity for the electron–phonon coupling, a sub-diffusive dynamic takes place in the present DNA single strand model.

Before concluding, we perform now a scaling analysis similar to that used in [45]. To do that, we considered that the complete electronic wave-packet can be divided in two parts:

(a) a small fraction around the initial position, i.e. with the return probability behaving as $c_{n<n_0}(t) \propto t^{-nu}$, where n_0 represents few sites;

(b) a power-law tail up to a cutoff distance x_m from the initial position (after this cutoff distance, an exponential decay takes place).

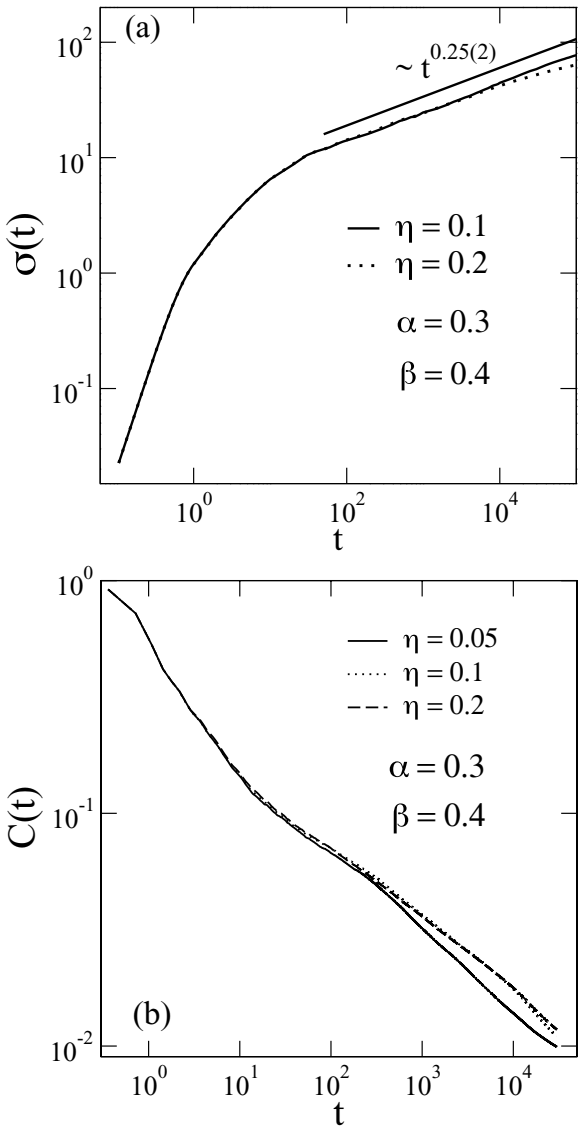

Figure 3. (*a*) Mean-square displacement $\sigma(t)$ and (*b*) temporal auto-correlation function $C(t)$ versus t for several values of the anharmonicity $\eta = 0.05$ up to 0.2 (unit is given in the main text). The off-diagonal electron–phonon coupling strength α was considered equal to 0.3, the highest intensity value at which we were able to get accurate numerical calculations. We observe that, even in the presence of weak cubic anharmonicity, the electron–phonon coupling promotes a sub-diffusive dynamics in a DNA single strand chain.

Therefore, x_m actually delimits the wave-packet front and evolves in time as $x_m \propto t^{\gamma}$, leading to [45]:

$$|c(t,n)|^2 \propto A_1 t^{-\nu} \quad \text{for} \quad n < n_0 \tag{14}$$

$$|c(t,n)|^2 \propto A_2 t^{-\gamma\phi} n^{-\phi} \quad \text{for} \quad n_0 < n < x_m \tag{15}$$

For a power-law tail $x^{-\phi}$ with $\phi > 1$, equation (15) does not contribute to the normalization of the wave-function. Hence equation (14) dominates, implying that we should have $\nu = 0$ in order to keep the complete electronic wave-packet normalized. This case with $\phi > 1$ was investigated in [45] and is completely distinct from the present case in which $\nu > 0$.

On the other hand, for $\phi < 1$ equation (15) will contribute to the normalization and hence we need to treat it as follows:

$$\int_0^{n_0} A_1 t^{-\nu} \mathrm{d}n = A_1 t^{-\nu} n_0 \;=\; \text{constant}. \tag{16}$$

To keep the wave-function normalized, n_0 should be proportional to t^{ν}. As a consequence, the electronic wave-packet can be summarized as:

$$|c(t,n)|^2 = \begin{cases} A_1 t^{-\nu} & \text{for} \quad 0 < n < n_0 \propto t^{\nu}, \\ A_2 t^{-\gamma\phi} n^{-\phi} & \text{for} \quad n_0 < n < x_m. \end{cases} \tag{17}$$

By using the scaling hypothesis of the previous equation, we can estimate analytically the time dependent behavior of the electronic wave-packet spread and the participation number. The participation number $\xi(t)$ can be written, in the continuous limit as:

$$\xi^{-1}(t) = \int_0^{n_0} A_1^2 t^{-2\nu} \mathrm{d}n + \int_{n_0}^{x_m} A_2^2 t^{-2\gamma\phi} n^{-2\phi} \mathrm{d}n, \tag{18}$$

leading to the following approximate expression:

$$\xi^{-1}(t) \propto C_1 t^{-2\nu} n_0 + C_2 t^{-2\gamma\phi} n_0^{1-2\phi}. \tag{19}$$

Using (16) we have:

$$\xi^{-1}(t) \propto C_1 t^{-\nu} + C_2 t^{-2\gamma\phi - 2\phi\nu + \nu}. \tag{20}$$

Therefore, the first term will dominate the dynamics, and the time-dependent behavior of the participation number is characterized by $\xi(t) \propto t^{\nu}$.

The electronic spread $\sigma(t)$ can be obtained in a similar way. In the continuous limit $\sigma^2(t)$ is given by :

$$\sigma^2(t) = \int_0^{n_0} A_1 t^{-\nu} n^2 \mathrm{d}n + \int_{n_0}^{x_m} A_2 t^{-\gamma\phi} n^{2-\phi} \mathrm{d}n. \tag{21}$$

The second integration is dominated by the limit $n = x_m$ yielding

$$\sigma^2(t) \propto A_1 t^{-\nu} n_0^3 + B_2 t^{-\gamma\phi} x_m^{3-\phi}. \tag{22}$$

Using (16) again together with the expression $x_m \propto t^{\gamma}$ we have:

$$\sigma^2(t) \propto A_1 t^{2\nu} + B_2 t^{\gamma(3-2\phi)} \tag{23}$$

The second term will dominate the time-dependence of the wave-packet spread leading to $\sigma(t) \propto t^{\gamma(3-2\phi)/2}$.

The next step is to check our scaling procedure by using our numerical calculations. In figure 4(*a*) we estimate the cutoff position x_m for times $t = 30\,000$ up to $180\,000$. Our best fit shows that $x_m \propto t^{\gamma}$, with $\gamma = 0.25(2)$. In figure 4(*b*) we plot the return probability ($R(t) = |c_{N/2}(t)|^2$) versus time. Our best fit shows that $R(t) \propto t^{-\nu}$ with $\nu = 0.20(2)$. Finally, in figure 4(*c*) we check our scaling hypothesis by collapsing the wave-function profile for distinct times in a single curve using $\phi = 0.5$, $\gamma = 0.25$, and $\nu = 0.2$, recovering the exponents of $\xi(t)$ and $\sigma(t)$ with good accuracy.

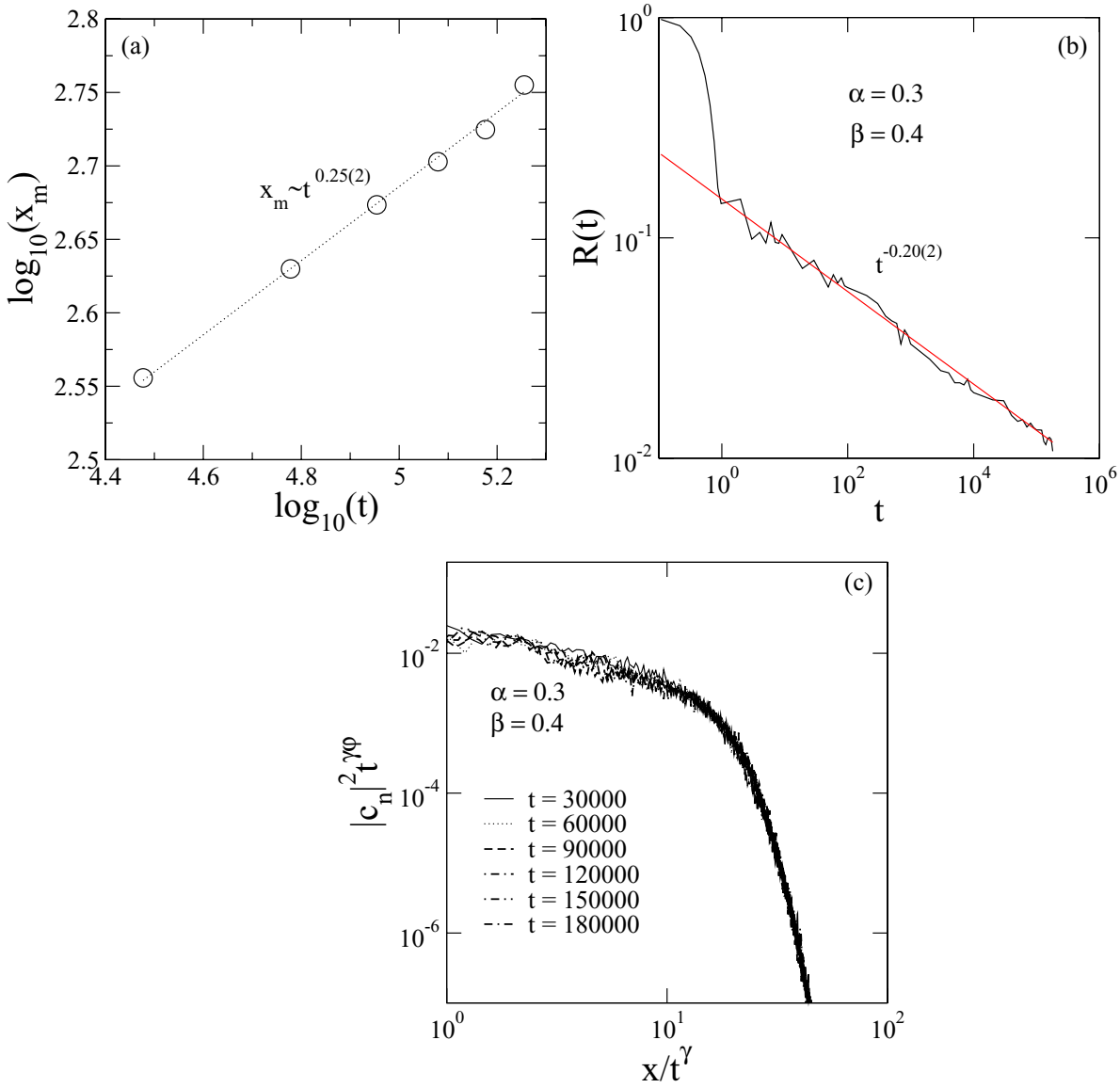

Figure 4. (*a*) Cutoff position x_m versus time for $t = 30\,000$ up to $180\,000$. Our best fit shows that $x_m \propto t^{\gamma}$ with $\gamma = 0.25(2)$. (*b*) The return probability ($R(t) = |c_{N/2}(t)|^2$) versus time. Our best fit shows that $R(t) \propto t^{-\nu}$ with $\nu = 0.20(2)$. (*c*) The data collapse of the wave-function profile for distinct times in a single curve with $\phi = 0.5$.

4. Summary and conclusions

In summary, we investigated the dynamics of a one-electron state moving in a finite DNA single-strand chain containing N bases considering, beyond the intrinsic DNA disorder distribution, the effect of the DNA's vibrations.

We treated the electronic dynamics by using a tight-binding one-electron Hamiltonian, and a classical harmonic Hamiltonian to describe the DNA's vibrations. The electron-lattice term was considered by assuming the electronic hopping energy dependent on the effective distance between the nearest-neighboring DNA's bases. Our analysis was done by tuning the electron–phonon coupling strength α as well as the harmonic spring constant β.

Our calculations revealed that the electron–phonon coupling can break down the Anderson localization, promoting the appearance of a sub-diffusive dynamics for long times. Furthermore, the effect of anharmonic corrections to the nearest-neighboring bases interaction was also taken into account by means of a cubic force similar to those considered in the Fermi–Pasta–Ulam model. The numerical result in the limit of weak anharmonicity corroborates that the electron–phonon coupling strength α indeed promotes a sub-diffusive wavepacket spread.

Acknowledgments

This work was partially financed by the Brazilian Research Agencies CAPES (PNPD), CNPq (INCT-Nano(Bio)Simes, Project no. 573925/2008-9 and Casadinho/Procad) and FAPEAL (Alagoas State Agency). The research work of MO Sales is supported by a graduate program sponsored by CAPES.

References

[1] Winfree E, Liu F, Wenzler L A and Seeman N C 1998 *Nature* **394** 539
[2] Porath D, Bezryadin A, De Vries S and Dekker C 2000 *Nature* **403** 635
[3] Xu B, Zhang P, Li X and Tao N 2004 *Nano Lett.* **4** 1105
[4] Kasumov Yu, Klinov D V, Roche P-E, Guéron S and Bouchiat H 2004 *Appl. Phys. Lett.* **84** 1007
[5] Yamada H 2004 *Int. J. Mod. Phys.* B **18** 1697
[6] Yamada H and Iguchi K 2010 *Adv. Condens. Matter Phys.* **2010** 380710
[7] Klotsa D, Römer R A and Turner M S 2005 *Biophys. J.* **89** 2187
[8] Shinwari M W, Deen M J, Starikov E B and Cuniberti G 2010 *Adv. Funct. Mater.* **20** 1865
[9] Endres R G, Cox D L and Singh R R P 2004 *Rev. Mod. Phys.* **76** 195
[10] Albuquerque E L, Fulco U L, Freire V N, Caetano E W S, Lyra M L and de Moura F A B F 2014 *Phys. Rep.* **535** 139
[11] Basko D M and Conwell E M 2002 *Phys. Rev.* B **66** 094304
[12] Conwell E M 2005 *Proc. Natl Acad. Sci.* **102** 8795
[13] Starikov E B 2005 *Phil. Mag.* **85** 3435
[14] Troisi A and Orlandi G 2002 *J. Phys. Chem.* B **106** 2093
[15] Maciá E 2007 *Phys. Rev.* B **76** 245123
[16] Senthilkumar K, Grozema F C, Fonseca Guerra C, Bickelhaupt F M, Lewis F D, Berlin Y A, Ratner M A and Siebbeles L A 2005 *J. Am. Chem. Soc.* **127** 14894
[17] Gutiérrez R, Mohapatra S, Cohen H, Porath D and Cuniberti G 2006 *Phys. Rev.* B **74** 235105
[18] Ren W, Wang J, Ma Z and Guo H 2006 *J. Chem. Phys.* **125** 164704
[19] Pikovsky A S and Shepelyansky D L 2008 *Phys. Rev. Lett.* **100** 094101
[20] de Moura F A B F, Gléria I, dos Santos I F and Lyra M L 2009 *Phys. Rev. Lett.* **103** 096401
[21] de Moura F A B F, Fulco U L, Lyra M L, Domínguez-Adame F and Albuquerque E L 2011 *Physica* A **390** 535
[22] Albuquerque E L, Vasconcelos M S, Lyra M L and de Moura F A B F 2005 *Phys. Rev.* E **71** 021910
[23] Albuquerque E L, Lyra M L and de Moura F A B F 2006 *Physica* A **370** 625
[24] Paéz C J, Rey-González R and schulz P A 2010 *Phys. Rev.* B **81** 024203
[25] de Moura F A B F 2013 *Physica* D **253** 66
[26] Brizhik L, Chetverikov A P, Ebeling W, Ropke G and Velarde M G 2012 *Phys. Rev.* B **85** 245105
[27] Hennig D, Velarde M G, Ebeling W and Chetverikov A P 2008 *Phys. Rev.* E **78** 066606
[28] Makarov V A, Velarde M G, Chetverikov A P and Ebeling W 2006 *Phys. Rev.* E **73** 066626
[29] Velarde M G 2010 *J. Comput. Appl. Math.* **233** 1432
[30] Su W P, Schrieffer J R and Heeger A J 1979 *Phys. Rev. Lett.* **42** 1698
[31] Su W P, Schrieffer J R and Heeger A J 1980 *Phys. Rev.* B **22** 2099
[32] Heeger A J, Kivelson S, Schrieffer J R and Su W P 1988 *Rev. Mod. Phys.* **60** 781
[33] Sales M O and de Moura F A B F 2014 *J. Phys.: Condens. Matter* **26** 415401
[34] Hairer E, Nϕrsett S P and Wanner G 2010 *Solving Ordinary Diferential Equations I: Nonstiff Problems* (*Springer Series in Computational Mathematics*) (Heidelberg: Springer)
[35] Press W H, Flannery B P, Teukolsky S A and Wetterling W T 2007 *Numerical Recipes: the Art of Scientific Computing* 3rd edn (Cambridge: Cambridge University Press)
[36] de Moura F A B F 2007 *Eur. Phys. J.* B **58** 389
[37] Sales M O and de Moura F A B F 2012 *Physica* E **45** 97
[38] de Moura F A B F, Coutinho-Filho M D, Lyra M L and Raposo E P 2004 *Europhys. Lett.* **66** 585
[39] Kawarabayashi T and Ohtsuki T 1995 *Phys. Rev.* B **51** 10897
[40] Chalker J T 1990 *Physica* A **167** 253
[41] Huckestein B and Schweitzer L 1994 *Phys. Rev. Lett.* **72** 713
[42] Kramer B and MacKinnon A 1993 *Rep. Prog. Phys.* **56** 1469
[43] Zavt G S, Wagner M and Lütze A 1993 *Phys. Rev.* E **47** 4108
[44] de Moura F A B F, Caetano R A and Santos B 2012 *J. Phys.: Condens. Matter* **24** 245401
[45] de Moura F A B F, Leão F F S and Lyra M L 2011 *J. Phys.: Condens. Matter* **23** 135303
[46] Dunlap D H, Wu H L and Phillips P W 1990 *Phys. Rev. Lett.* **65** 88